J Solid State Electrochem (2010) 14:835–840
DOI 10.1007/s10008-009-0862-x

ORIGINAL PAPER

Pt dendrimer nanocomposites for oxygen reduction reaction in direct methanol fuel cells

J. Ledesma-Garcia · I. L. Escalante-Garcia · Thomas W. Chapman · L. G. Arriaga · V. Baglio · V. Antonucci · A. S. Aricò · R. Ornelas · Luis A. Godinez

Received: 8 December 2008 / Revised: 26 April 2009 / Accepted: 6 May 2009 / Published online: 27 May 2009

Abstract Dendrimer-encapsulated Pt nanoparticles (G4OHPt) were prepared by chemical reduction at room temperature. The G4OHPt, with average diameters of ca. 2.7 nm, were characterized by X-ray diffraction, scanning electron microscopy, and thermogravimetric analysis. Electrocatalytic behavior for oxygen reduction reaction was investigated using a rotating disk electrode configuration in an acidic medium, with and without the presence of methanol (0.01, 0.1, and 1 M). Kinetic studies showed that electrodes based on Pt nanoparticles encapsulated inside the dendrimer display a higher selectivity for ORR in the presence of methanol than electrodes based on commercial Pt black catalysts. Also, the dendritic polymer confers a protective effect on the Pt in the presence of methanol, which allows its use as a cathode in a direct methanol fuel cell operating at different temperatures. Good performance was obtained at 90 °C and 2 bar of pressure with a low platinum loading on the electrode surface.

J. Ledesma-Garcia · I. L. Escalante-Garcia · T. W. Chapman · L. G. Arriaga · L. A. Godinez (✉)
Centro de Investigación y Desarrollo Tecnológico en Electroquímica, Parque Tecnológico Querétaro, Sanfandila, Pedro Escobedo, C. P., 76703 Querétaro, Mexico
e-mail: lgodinez@cideteq.mx

V. Baglio · V. Antonucci · A. S. Aricò
CNR-ITAE,
Via Salita S. Lucia sopra Contesse 5,
98126 Messina, Italy

R. Ornelas
Tozzi Renewable Energy SpA,
Via Zuccherificio, 10,
48010 Mezzano (RA), Italy

Keywords Oxygen reduction reaction · Direct methanol fuel cells · Dendrimer-encapsulated platinum nanoparticles

Introduction

Direct methanol fuel cells (DMFCs) are considered a potential alternative power source for portable applications due to both superior specific energy density when compared to the best rechargeable battery and to their operational capabilities at low temperature and pressure [1–3].

The best known catalyst for oxygen reduction reaction (ORR) is Pt, and great efforts have been made to improve its utilization and activity. However, in the presence of methanol, it displays a formation of mixed potentials, which leads to lower current densities as well as a decrease in the overall efficiency of the cell [4, 5]. One approach consists of developing new electrocatalysts for ORR which, at the same time, shows both a high tolerance to methanol coming from the anode (through the membrane) and high electrocatalytic activity for ORR [2, 5–7]. In this context, platinum alloys with transition metals have been proposed to counteract the methanol effect and to achieve acceptable cathodic current densities for ORR [8–12].

The efficient use of Pt and new methods of preparing better electrocatalysts that are selective for O_2 and tolerant to methanol are still being sought. Hence, the goal is to develop Pt electrocatalysts with nanometric particle size, a defined shape, and high-dispersion, all of which would allow high electrocatalytic activity for ORR [13, 14].

A method recently reported [15, 16] to prepare monometallic and bimetallic nanoparticles uses organic macromolecules as support, specifically dendrimers, and could be

an alternative approach to achieving the electrocatalytic properties that researchers are looking for in Pt. These hybrid nanocomposites, comprised of metallic particles within an organic matrix, are applied to homogenous and heterogenous catalysis [17–20]. The internal cavities of the dendritic macromolecules, highly branched, perform as nanoreactors for the syntheses and stabilization of transition metallic particles of nanometer size [21]. In general, the dendrimers are recognized for their ability to control the arrangement and composition of their interior/exterior functional groups. In addition, their particular macromolecular architecture creates interior spaces and an ideal environment for trapping desired guest species and, simultaneously, excluding other species from the interior. Also, the peripherical functional groups are immobilized on conductive surfaces such as carbon materials, ITO-coated glass, Au, and others [18, 22–25]. Hence, the Pt-dendrimer-encapsulated nanoparticles provide attractive structural features as nanoelectrocatalysts for constructing electrodes for fuel cell applications [26–28].

In the present study, the effect of methanol on Pt nanoparticles encapsulated in a hydroxyl-terminated generation 4.0 PAMAM dendrimer anchored to oxidized-carbon surfaces like cathodes in a DMFC is described. The electrochemical behavior of G4OHPt for ORR was investigated by cyclic voltammetry (CV) and rotating disk electrode (RDE) in the presence of methanol in an acidic solution and compared to Pt black commercial catalysts. Furthermore, the electrocatalytic activity of these materials was studied in a DMFC system in order to confirm the half-cell results. The results reveal that the dendritic polymer offers an interesting protective effect to the Pt nanoparticle in the presence of methanol at low concentrations.

Experimental

Synthesis and characterization of catalysts

The dendrimer-encapsulated Pt nanoparticles were prepared from 6 mM K_2PtCl_4 solution (99.99%, Strem Chemicals) and 0.1 mM hydroxyl-terminated PAMAM dendrimer Generation 4 (G4OH, 10 wt.% in methanol from Aldrich) aqueous solution. The mixture was stirred constantly for 48 h in the dark. Consequently, an excess of $NaBH_4$ was added as reducing agent [29]. The final solution (G4OHPt) was purified by dialysis (benzoylated cellulose-membrane tubing, cut-off 1,200 Da, Sigma-Aldrich) and then used in the preparation of electrodes.

The catalyst obtained was characterized by X-ray diffraction (XRD) patterns from films of G4OHPt deposited onto a Si substrate using a Philips X-Pert 3710 diffractometer [23]. The peak profile of the 111 reflection in the face-centered cubic structure was obtained by using the Marquardt algorithm and used to calculate crystallite size using the Debye–Scherrer equation [30]. The result was confirmed via scanning electron microscopy (SEM) analysis on a Philips XL 30 Scanning electron microscope. In addition, thermogravimetric analysis (TGA) experiments were carried out on an STA 409C of NETZSCHE-Gerätebau GmbH Thermal Analysis. Weight changes were recorded as a function of temperature for a 5 °C/min ramp between room temperature and 450 °C in air atmosphere.

Half-cell experiments

Glassy-carbon rotating disk electrodes (GCE, Bioanalytical Systems, 3.0 mm diameter) were used as working electrodes. Their surfaces were polished using alumina powder on a polishing cloth (Buehler) until a mirror finish was obtained. This was followed by immersion in an ultrasonic bath in isopropanol and water for 10 min each, respectively. After rinsing with plenty of water, the GCEs were pretreated anodically in aqueous 0.5 M H_2SO_4. Later, the functional surfaces were modified with G4OHPt by electrochemical immobilization in 0.1 NaF (J.T. Baker) according to published procedures [23, 31]. For comparison, a commercial Pt black (Johnson Matthey) catalyst was used. The catalyst was dispersed in a mixture of 15 wt.% Nafion® solution and deionized water and deposited on previously prepared GCE.

Cyclic voltammetry and RDE measurements were carried out in a standard-three electrode cell where a Pt wire and Hg/Hg_2SO_4 electrode served as the counter and reference electrodes, respectively. Potentials reported here are referred to a normal hydrogen electrode (NHE). ORR was studied in pure oxygen-saturated 0.5 M H_2SO_4 and after in the presence of 0.01, 0.1, and 1 M methanol. CV experiments were carried out at a scan rate of 50 mV s^{-1}. Current–potential curves were recorded at a 10 mV s^{-1} linear scan rate and different rotation rates at 30 and 60 °C with an Epsilon potentiostat from Bioanalytical Systems. In addition, a BASi RDE-2 was used as the rotator system.

DMFC measurements

Commercial gas diffusion backing layers [(GDL), HT ELAT, E-Tek] were used to prepare the electrodes. The catalyst in the cathodic compartment was constructed from layers of solid G4OHPt on GDL prepared by solvent evaporation (Pt loading 0.5 mg cm^{-2}). In the anode, a mixture formed by a commercial Pt-Ru black (Alfa Aesar, 50:50 atomic ratio, 6 mg cm^{-2}) catalyst,

15 wt.% Nafion, and isopropanol was spread on the GDL. A Nafion 117 (DuPont) was used as the electrolyte. For comparison, a catalytic layer based on a Pt black catalyst (Johnson Matthey) with 15 wt.% Nafion was spread on the GDL using a Pt loading of 5 mg cm^{-2}. Membrane-electrode assemblies were formed by a hot-pressing procedure [32] and located in a fuel cell test fixture with a 5 cm^2 active area. The fuel cell was then connected to the test station, including an HP60606B electronic load. After, 1 M aqueous methanol (2 ml min^{-1}) and oxygen (about 300 ml min^{-1}), pre-heated to the same temperature of the cell, were fed to the anodic and cathodic compartments of the DMFC, respectively. Single-cell performance was investigated by steady-state galvanostatic polarization measurements.

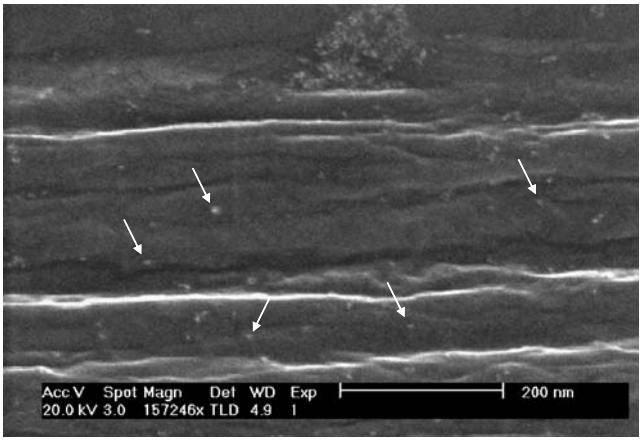

Fig. 1 SEM of G4OHPt catalyst anchored to GDL

Results and discussion

Physicochemical characterization of G4OHPt

Results obtained from the XRD analysis of G4OHPt are presented in Table 1. The Pt nanoparticles show a face-centered-cubic crystallographic structure typical of Pt. The lattice parameter is close to that reported for Pt-based materials [33]. Crystallite size was calculated using the Scherrer equation; it was confirmed by SEM images of the G4OHPt anchored to the GDL presented in Fig. 1. Average particle size is in the range of 2 to 3 nm.

In order to investigate the stability of dendrimer-Pt-based catalysts in relation to temperature, a thermal analysis was carried out (not shown). The results of TGA showed that the catalyst loses 5% of its initial weight at 200 °C. According to Ozturk and coworkers [34], these changes correspond to the rupture of amides present in the structure of the dendrimer. Major changes occur in the range of 200 to 300 °C due to the dendrimer loss from the catalyst [34].

Electrochemical characterization

Figure 2 shows the voltamperometric response of unmodified and G4OHPt-modified GCEs in 0.5 M H_2SO_4 measured in a potential range of 0 to 1.3 V vs. NHE at 30 °C. The typical voltammetric curve of Pt [4] is observed in Fig. 2—II. Hydrogen adsorption/desorption peaks as well as the PtO formation/reduction are easily identified.

Table 1 Physicochemical characteristics of dendrimer-encapsulated Pt nanoparticles (G4OHPt)

Average particle size/ nm (XRD)	Lattice parameter/ nm (XRD)	Inter-atomic distance/nm (XRD)	Average of particle size/nm (SEM)
2.7	0.39207	0.1386	2–3

The electrochemical surface area (ESA) was estimated from the charge (Q_H=210 μC cm^{-2}) to oxidize a full monolayer of adsorbed hydrogen atoms. The specific surface area (103.77 m^2 g^{-1}), calculated from the ESA/Pt loading ratio [35], was comparable to commercial Pt/C based catalysts [23].

Figure 3 compares the voltammograms of a G4OHPt-modified GCE measured in 0.5 M H_2SO_4 in the presence of different methanol concentrations under N_2–atmosphere and 30 °C. The curves show adequate tolerance to the presence of MeOH when the MeOH concentration is 0.01 and 0.1 M. A methanol oxidation peak is observed in both forward and reverse scans using 1 M methanol. In the forward scan, the methanol oxidation

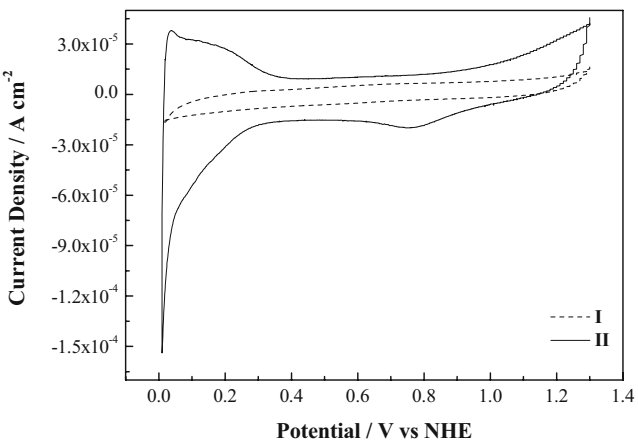

Fig. 2 Cyclic voltammograms of (*I*) clean and (*II*) G4OHPt-modified GCE in N_2-purged 0.5 M H_2SO_4 at 30 °C and 50 mV s^{-1} of scan rate

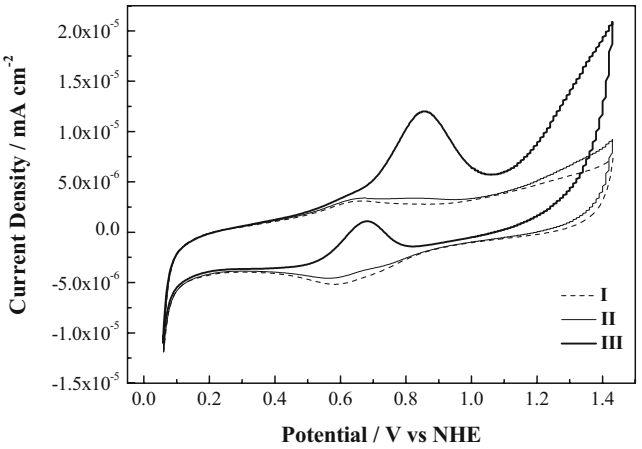

Fig. 3 Cyclic voltammograms of G4OHPt-modified GCE in N_2-purged 0.5 M H_2SO_4+ (*I*) 0.01, (*II*) 0.1, and (*III*) 1 M of methanol at 30 °C. Scan rate of 50 mV s^{-1}

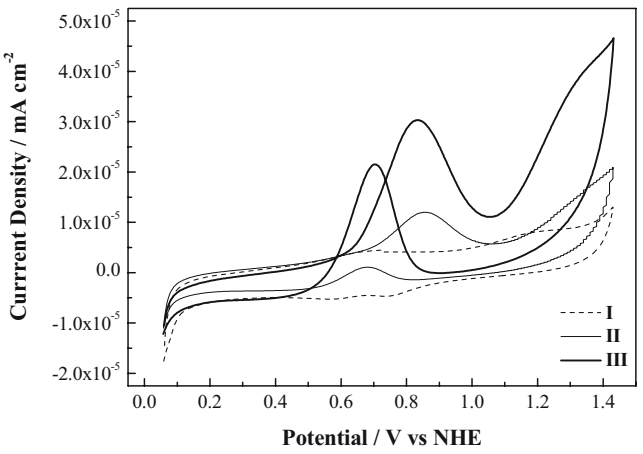

Fig. 5 Cyclic voltammograms of G4OHPt-modified GCE in N_2-purged 0.5 M H_2SO_4+ (*I*) 0.01, (*II*) 0.1, and (*III*) 1 M of methanol at 60 °C. Scan rate of 50 mV s^{-1}

peak occurs at approximately 0.85 V [36]. This result suggests that the complex structure of the dendritic molecules prevents the entrance of methanol, conferring a protective effect on the encapsulated Pt nanoparticle. When the concentration of alcohol is increased, the gradient between the internal micro-ambient of the dendrimer and the dissolution bulk promotes the incursion of alcohol through the Pt surface, where it is oxidized.

Polarization curves for ORR on G4OHPt-modified GCE in oxygen-saturated acid media at 1,600 rpm and 30 °C in both the absence and presence of methanol are shown in Fig. 4. The performance of this catalyst for ORR remains practically constant in both the absence and presence of 0.01 and 0.1 M of methanol. However, when the concentration of methanol is high, especially in the activation controlled region (0.7–0.95 V vs. NHE), performance declines. A shift in the potential of approximately 80 mV (at 28 μA cm^{-2}) between curves I and IV is observed, together with a decrement in limiting current density (Fig. 4). This result is supported by the cyclic voltammetry data presented above.

In order to understand the protective effect of the dendrimer on Pt nanoparticles in the presence of methanol, cyclic voltammetry experiments at 60 °C were carried out. According to cyclic voltammograms presented in Fig. 5, the oxidation of methanol on G4OHPt-modified GCE occurs at 0.1 M, while at 30 °C,

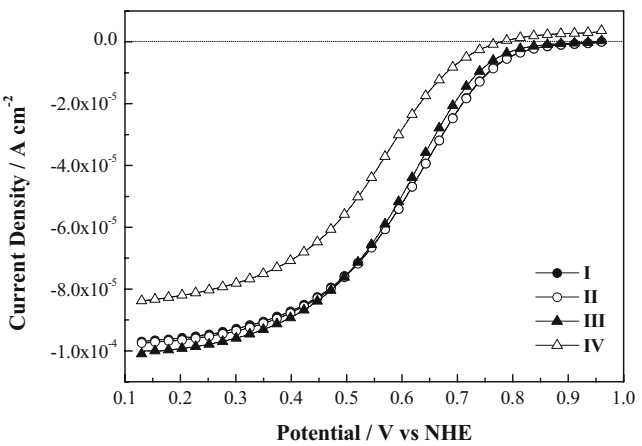

Fig. 4 Current–potential profiles for ORR on G4OHPt-modified GCE in O_2-saturated 0.5 M H_2SO_4 in the absence (*I*) and the presence of methanol: (*II*) 0.01, (*III*) 0.1, and (*IV*) 1 M at 30 °C and 1,600 rpm. Scan lineal rate of 10 mV s^{-1}

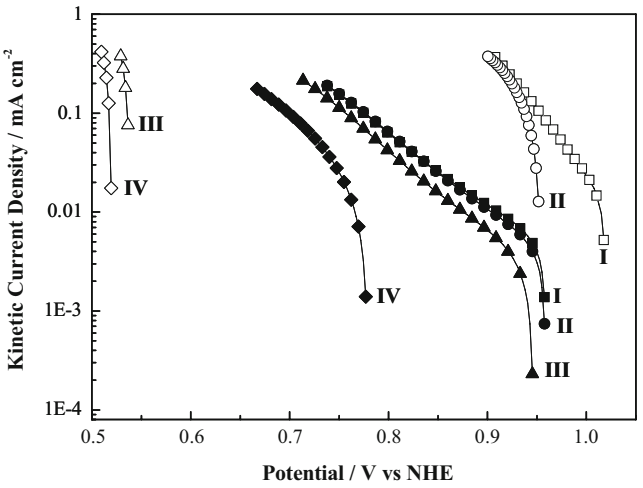

Fig. 6 Tafel plots corrected for mass transfer for ORR on G4OHPt-modified GCE and Pt black catalyst in 0.5 M H_2SO_4 in the presence of different concentrations of methanol: (*I*) 0, (*II*) 0.01, (*III*) 0.1, and (*IV*) 1 M. *Black marks* correspond to G4OHPt and *white marks* to the commercial catalyst

it occurs at 1 M. This suggests that the incursion of methanol through the Pt surface is facilitated by an expansion of the globular structure of the dendrimer, which results from incremental of temperature [37]. Hence, the protective effect of radial polymer on metallic nanoparticles could diminish at higher temperatures.

The electrocatalytic activity of G4OHPt-modified GCE for ORR was evaluated by rotating disk electrode measurements at different rotation rates, from 100 to 1,600 rpm in O_2-saturated aqueous 0.5 M H_2SO_4/CH_3OH solutions at 30 °C. Catalytic activity of G4OHPt-modified GCE surfaces for ORR was compared to that of the Pt Black (Johnson Matthey) commercial catalyst. The data recorded from the polarization curves for ORR were used to get mass-transfer-corrected Tafel plots in order to evaluate kinetic behavior [38, 39]. Figure 6 shows the mass-transfer corrected Tafel plots for ORR on G4OHPt-modified GCE and Pt black in O_2-saturated 0.5 M H_2SO_4 in both the absence and the presence of methanol.

The formation of a mixed potential, due to the simultaneous reaction of methanol oxidation and oxygen reduction in the same potential range, causes a shift toward lower potentials when methanol concentration is increased. However, the shift in potential is 74 mV (at 0.128 mA cm^{-2}) for the G4OHPt-modified GCE and 430 mV for the commercial catalyst measured at the same current density. This clearly indicates that the encapsulated Pt nanoparticles promote ORR in the presence of methanol as a result of the protective effect of the dendrimer.

Polarization and power density curves for DMFCs equipped with G4OHPt and Pt black cathode catalysts at different temperatures and 2 bar of pressure in the cathode compartment were recorded. Figure 7 shows the maximum power density plot as a function temperature for a cell equipped with G4OHPt as the cathode catalyst. Better performance of the DMFC was obtained at 90 °C and 2 bar of pressure. This performance was compared to that of a commercial catalyst in Fig. 8. The Pt black-based cell performs largely better than the cell equipped with G4OHPt as the cathode catalyst at 90 °C. In fact, power density is 180 mW cm^{-2} for Pt black, whereas it is 56 mW cm^{-2} for G4OHPt. It is important, however, to point out that a very low Pt loading was used at the cathode of the G4OHPt-based cell (0.5 mg cm^{-2}), one approximately ten times lower than that used in a commercial catalyst-based cell (5 mg cm^{-2}).

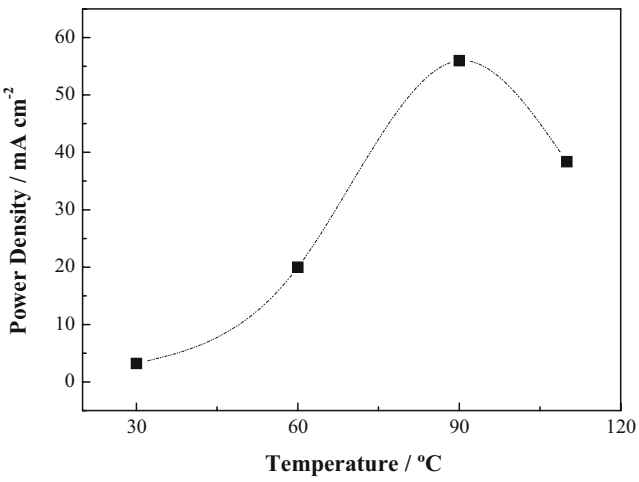

Fig. 7 Relationship between the maximum power density values and the operational temperature of the DMFC equipped with G4OHPt as cathode

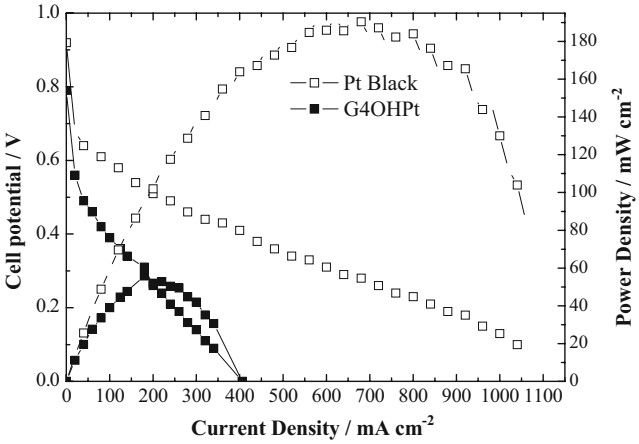

Fig. 8 Polarization and power density plots for the DMFCs equipped with G4OHPt and Pt black as cathode catalysts at 90 °C, under 2 bar of pressure

Conclusions

Dendrimer-encapsulated Pt nanoparticles were prepared and physicochemically characterized by XRD and SEM techniques. Electrocatalytic behavior for ORR was investigated in RDE configuration in an acidic medium in both the absence and presence of methanol. The dendritic polymer prevents the interference of methanol, at low concentrations, with the Pt nanoparticle surface, preventing, thus, Pt poisoning. This effect allowed the use of Pt nanoparticles as cathodic catalysts in DMFCs operating at different temperatures.

Acknowledgments This study was supported by The Mexican Council for Science and Technology (CONACyT, Grant 45517). L-G J and E-G IL are grateful to CONACyT for graduate fellowships. Arriaga LG expresses thanks to The Mexican Council for Science and Technology (Conacyt, SEP-Conacyt 61067).

References

1. Zhong S, Cui X, Cai H, Fu T, Zhao C, Na H (2007) J Power Sources 164:65. doi:10.1016/j.jpowsour.2006.10.077
2. Chu D, Jian R (2002) J Electrochem Soc 148:591
3. Dillon R, Srinivasan S, Arico AS, Antonucci V (2004) J Power Sources 127:112. doi:10.1016/j.jpowsour.2003.09.032
4. Gasteiger HA, Marković N, Ross PN, Cains EJ (1993) J Phys Chem 97:12020. doi:10.1021/j100148a030
5. Gilman S, Chu D (2003) In: Vielstich W, Lamm A, Gaister HA (eds) Handbook of fuel cells: fundamentals, technology and application. Wiley, New York
6. Eickes C, Piela P, Davey J, Zelenay P (2006) J Electrochem Soc 153:A171. doi:10.1149/1.2136073
7. Liu Z, Ling XY, Su X, Lee JY (2004) J Phys Chem B 108:8234. doi:10.1021/jp049422b
8. Baglio V, Aricó AS, Stassi A, D'Urso C, Di Blasi A, Castro Luna AM, Antonucci V (2006) J Power Sources 159:900. doi:10.1016/j.jpowsour.2005.12.088
9. Yang H, Alonso-Vante N, Lamy C, Akins DL (2005) J Electrochem Soc 152:A704. doi:10.1149/1.1862258
10. Xiong L, Manthiram A (2005) J Electrochem Soc 152:A697. doi:10.1149/1.1862256
11. Baglio V, Stassi A, Di Blasi A, D'Urso C, Antonucci V, Aricò AS (2007) Electrochim Acta 53:1361. doi:10.1016/j.electacta.2007.04.099
12. Baglio V, Di Blasi A, D'Urso C, Antonucci V, Aricò AS, Ornelas R, Morales-Acosta D, Ledesma-Garcia J, Godinez LA, Morales-Alvarez L, Arriaga LG (2008) J Electrochem Soc 155:B829. doi:10.1149/1.2938368
13. Kinoshita K (1992) Electrochemical oxygen technology. Wiley, Hoboken
14. Takasu Y, Kawaguchi T, Sugimoto W, Murakami Y (2003) Electrochim Acta 48:3861. doi:10.1016/S0013-4686(03)00521-8
15. Zhao M, Sun L, Crooks RM (1998) J Am Chem Soc 120:4877. doi:10.1021/ja980438n
16. Balogh L, Tomalia DA (1998) J Am Chem Soc 120:7355. doi:10.1021/ja980861w
17. Scout RW, Wilson OM, Crooks RM (2005) J Phys Chem B 109:692. doi:10.1021/jp0469665
18. Ye H, Crooks RM (2007) J Am Chem Soc 129:3627. doi:10.1021/ja068078o
19. Ledesma-García J, Escalante-Garcia IL, Chapman TW, Rodríguez FJ, Godínez LA (2006) ECS Trans 3:12
20. Escalante-Garcia IL, Ledesma-Garcia J, Chapman TW, Godinez LA (2008) ECS Trans 11:43. doi:10.1149/1.2953505
21. Knecht MR, Wright DW (2004) Chem Mater 16:4890. doi:10.1021/cm049058t
22. Vijayaraghavan G, Stevenson KJ (2007) Langmuir 23:5279. doi:10.1021/la0637263
23. Ledesma-Garcia J, Escalante-Garcia IL, Rodríguez FJ, Chapman TW, Godínez LA (2008) J Appl Electrochem 38:515. doi:10.1007/s10800-007-9466-2
24. Crespilho FN, Huguenin F, Zucolotto V, Olivi P, Nart FC, Oliveira ON Jr (2006) Electrochem Commun 8:348. doi:10.1016/j.elecom.2005.12.003
25. Raghu S, Nirmal RG, Mathiyarasu J, Berchmans S, Phani KLN, Yegnaraman V (2007) Catal Lett 119:40. doi:10.1007/s10562-007-9154-1
26. Ledesma-Garcia J, Barbosa R, Chapman TW, Arriaga LG, Godinez LA (2009) Int J Hydrogen Energy 34:2008. doi:10.1016/j.ijhydene.2008.11.106
27. Raghu S, Berchmans S, Phani KLN, Yegnaraman V (2007) Chem Asian J 2:775. doi:10.1002/asia.200700013
28. Maiyalagan T (2008) J Solid State Electrochem. doi:10.1007/s10008-008-0730-0
29. Crooks RM, Zhao M, Sun L, Chechik V, Yeung LK (2001) Acc Chem Res 34:181. doi:10.1021/ar000110a
30. Uvarov V, Popov I (2007) Mater Charact 58:883. doi:10.1016/j.matchar.2006.09.002
31. Ye H, Crooks RM (2005) J Am Chem Soc 127:4930. doi:10.1021/ja0435900
32. Aricò AS, Shukla AK, el-Khatib KM, Cretì P, Antonucci V (1999) J Appl Electrochem 29:671. doi:10.1023/A:1003538230286
33. Murthi VS, Urian RC, Mukerjee S (2004) J Phys Chem B 108:11011. doi:10.1021/jp048985k
34. Ozturk O, Black TJ, Perrine K, Pizzolato K, Williams CT, Parsons FW, Ratliff JS, Gao J, Murphy CJ, Xie H, Ploehn HJ, Chen DA (2005) Langmuir 21:3998. doi:10.1021/la047242n
35. Thompson SD, Jordan LR, Forsyth M (2001) Electrochim Acta 46:1657. doi:10.1016/S0013-4686(00)00767-2
36. Aricò AS, Baglio V, Di Blasi A, Modica E, Monforte G, Antonucci V (2005) J Electroanal Chem 576:161. doi:10.1016/j.jelechem.2004.10.014
37. Vögle F, Gestermann S, Hesse R, Schwierz H, Windisch B (2000) Prog Polym Sci 25:987. doi:10.1016/S0079-6700(00)00017-4
38. Gileadi E (1993) Electrode kinetics for chemists, chemical engineers and materials scientists. Wiley-VCH, New York
39. Bard AJ, Faulkner L (1980) Electrochemical methods. Wiley, New York